Aalborg Universitet

AALBORG UNIVERSITY

Glucose-insulin mathematical model for the combined effect of medications and life style of Type 2 diabetic patients

Ahdab, Mohamad Al; Leth, John; Knudsen, Torben; Vestergaard, Peter; Clausen, Henrik Glavind

Link to publication from Aalborg University

Regular article

Glucose-insulin mathematical model for the combined effect of medications and life style of Type 2 diabetic patients[☆]

Mohamad Al Ahdab [a],[*], John Leth [a], Torben Knudsen [a], Peter Vestergaard [b], Henrik Glavind Clausen [a]

[a] Section of Automation and Control, Department of Electronic Systems, Aalborg University, DK-9220 Aalborg Øst, Denmark
[b] Steno Diabetes Center North Jutland, Aalborg, Denmark

A R T I C L E I N F O

A B S T R A C T

The goal of this paper is to propose a new mathematical model for the combined effect of different treatments and lifestyles on the glucose-insulin dynamics of Type 2 diabetes (T2D) patients. The model gives the possibility to take into consideration physical activity, stress, meals, and medications while evaluating or designing treatment plans for T2D patients. The model is proposed by combining and modifying some of the available models in the literature. Simulations were performed for the modifications to show how the model confirm with literature on T2D patients. Additionally, a discussion is provided to demonstrate the ability of the model to be used in the assessment of treatment plans and in the design for robust insulin dose guidance algorithms. An open source code for the model is additionally provided.

1. Introduction

One of the greatest health challenges which faces humanity in the 21st century is the emergence of type 2 diabetes (T2D) as a global pandemic. More than 463 million were reported to suffer from diabetes in 2019 and the number is expected to reach 700 million by 2045 [15]. Moreover, the global expenses related to diabetes are estimated to be 760 billion USD in 2019 and they are expected to increase [15]. T2D is characterized by high levels of glucose concentration in the blood. This increase in glucose levels can cause cardiovascular, kidney, and eye diseases and, if left untreated, will lead to organ failures. For T2D patients, low sensitivity to insulin, which is the hormone responsible for lowering glucose concentration in the blood, causes the beta cells in the pancreas to produce insulin to compensate. This will eventually weaken the cells and damage them, which in turn will make the body fail to regulate glucose concentration [24]. Insulin based treatment is initiated at later stages of the T2D disease when changes in diets and physical activities accompanied with oral medications have failed. Clinically, it is difficult to calculate suitable insulin doses and oral medication treatment plans for each specific patient. Therefore, many patients experience uncontrolled hyperglycemia for a long period of time until they

reach a safe level of glucose [38]. Having a model to simulate the combined effect of oral medications, insulin doses, and lifestyle changes can help medical professionals in the evaluation of different treatment plans. Moreover, such models can be used together with robust control methods to design automatic insulin guidance algorithms that ensure safe reach to the desired glucose concentrations.

In general, there are two main categories of methods to model systems: first principles methods, or data driven methods derived by fitting data to general mathematical structures such as ARMAX models.

The glucose-insulin dynamical models for T2D patients based on first principles can vary with different degrees of complexity. In the literature, there exist two main categories of such models: minimal models and maximal models [7]. Maximal models are very detailed models, which model metabolic functions at a molecular level. On the other hand, minimal models are less detailed and rely mostly on compartments and mass balance equations. While maximal models provide a great level of accuracy, the amount of different data, which is required to estimate parameters for these models is large and difficult to obtain from patients undergoing typical treatment plans. Moreover, the high accuracy of maximal models provides little relevance to the accuracy of the general glucose-insulin dynamics within the human body [7].
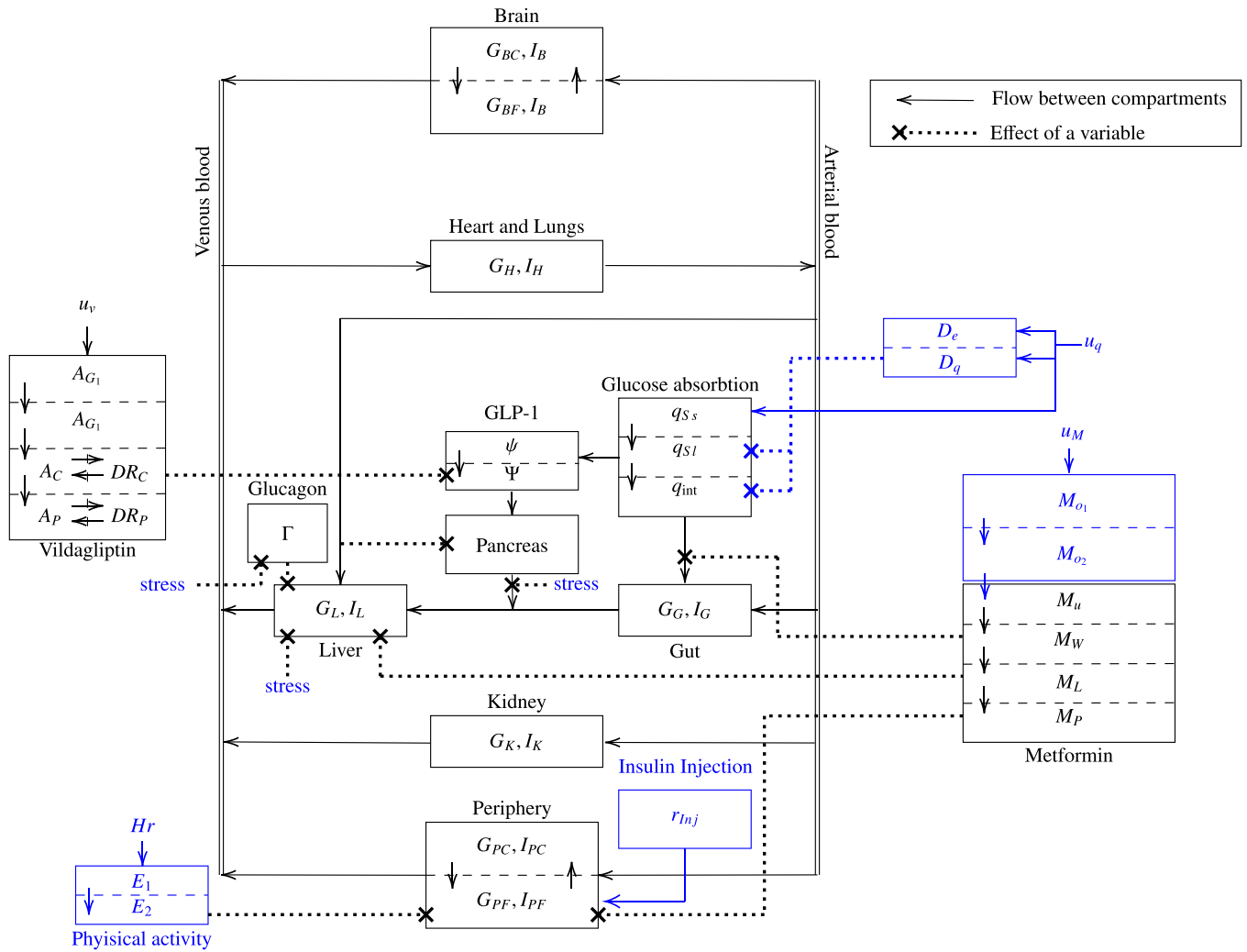

Fig. 1. A summary of the overall model with blue indicating the modified or added models compared to [10].

In contrast, minimal models consist of compartments to represent the distribution, diffusion, and production of glucose and insulin in the body with terms to represent the interaction between them. Furthermore, these models include pharmacokinetic equations to describe exogenous insulin injections and the intake of other medications. Several mathematical structures have been developed for the glucose-insulin dynamics in T2D patients. Some of them have a simple structure with less than ten states such as the ones presented in [2,31]. These models consider simple insulin injections and meal models. Their simplicity make them good candidates for patient specific parameter estimation and control design. Nevertheless, the few number of states force them to consider generic insulin and glucose states without considering other metabolic hormones (e.g. glucagon). Thus, making the process of augmenting them with oral medications and stress difficult. On the other hands, the models in [35,36] are larger and more complex. The model in [36] has recently been proposed and confirmed with patient data. Parameters were estimated as mean and covariance matrices of a normal distribution from patients' data. Only the mean and the diagonal elements of the covariance matrices were reported. The model includes a glucose ingestion model that takes into account only glucose meal given after fasting conditions. The model was also augmented with an insulin degludec linear pharmacokinetic model in [37]. As for the model in [35], it is based on [33] and includes the effect of oral medications (metformin and vildagliptin), Glucagon, and Glucagon-like peptide-1. The model uses the same glucose ingestion model from [36] and it is only for glucose meals after fasting conditions. Only mean parameters were reported. The work in [11] focused on the glucose dynamics in the brain and

provided a mathematical description for the effect of stress in diabetic patients. Physical activity has been modelled before but mainly for type 1 diabetes patients. It has been included in simple models such as the one in [6,29] or more complicated ones such as the one in [8].

Heart beat rate data from smart watches [30] and data regarding stress levels from self-assessment questionnaires [1,26] are becoming more feasible to be obtained from patients during treatment. Therefore, having a model to simulate the combined effect of different types of treatments together with the effect of stress and physical activity can improve the process of evaluating and developing treatment plans for diabetic patients.

Therefore, in this work, it is intended to present a mathematical structure for the combined effect of multiple glucose meals with no fasting conditions, insulin injections, multiple oral doses of metformin with different sizes, physical activity, and stress. Additionally, a Matlab [25] toolbox is developed to simulate patients is provided as an open source code on GitLab[1] for others to use the model easily and have a better chance to contribute for the development of the model. This structure can help with analyzing treatment plans depending on lifestyle conditions. Moreover, the structure can be used with robust control strategies to obtain algorithmic insulin dose calculators The structure is based on the one in [10] with modifications and inclusions as following (see Fig. 1): .

---

[1] https://gitlab.com/aau-adapt-t2d/aau-t2d-simulator.

- Modifying the model to account for multiple meals (see Section 2.1).
- Including a model for insulin injections based on [23] (see Section 2.2).
- Modifying the metformin model to account for multiple different doses in Section 2.3.
- Including the effect of physical activity based on [6] (see Section 2.4).
- Including the effect of stress based on [11] (see Section 2.5).

In addition, a discussion on how the developed model can be used, and what type of data is needed to fit the model is provided in Section 3. All simulations are performed using the toolbox from GitLab. The model parameters, which are used in the simulations, are found in Table B.3.

2. Model description

The model is mainly based on the one from [10] with the following four main subsystems: .

- Glucose subsystem.
- Insulin subsystem.
- Glucagon subsystem.
- Incretins hormone subsystem.

See Fig. 1 for an overview of the model. The glucose and insulin subsystems are modelled as a set of compartments representing different main parts of the human body: brain, heart and lungs, guts, liver, kidney, and peripherals. The flow between these compartments follows the human blood cycle. As for the glucagon and the incretins, a single compartment is used for each one of them as it is assumed that glucagon and incretins have equal concentration in all the body parts. In addition, the model contains metabolic production and uptake rates for different compartments. These metabolic rates are generally defined as their basal values multiplied with scaling variables that depend on the concentrations of insulin, glucose, and/or glucagon (see (A.1)). The pancreas has a different nonlinear and hybrid model. In addition, a glucose ingestion model based on [9] is included as in [35] but modified to handle multiple meals along the day. Moreover, metformin and vildagliptin oral treatment models are included based on [34] and [21] respectively, as in [10] but with a modification on the oral metformin model to handle different oral doses along the treatment. Additionally, a physical activity model based on [6] is added to the model. Furthermore, long acting and fast acting insulin injection models based on [23] are added. Finally, stress is included as a factor $\alpha_s \in [0,1]$ as in [11]. The main model includes parameters that were estimated by [33] for a healthy 70 kg male. The work in [35] considered a subset of these parameters to be estimated for the diabetic cases. Parameters for the different added models are taken from their corresponding literature.

In the following subsections, the added and modified models and states will be discussed. The full model equations are provided in Appendix A.

2.1. Glucose absorption model

In this section, a modification is introduced to account for multiple glucose meal sizes. The model is based on the one used in [35] which is based on [9]. The model takes into account that the gastric emptying of the stomach is correlated with the stomach content; which is supported by the study in [14]. The model in [35] and [9], however, are used for oral glucose tolerant tests only. The aim in this section is to make the model to take into account the effect of accumulated glucose meals on gastric emptying. It is acknowledged that gastric emptying depends on many factors other than the size of the meal as described in [17] and there exist models, which focus primarily on meal ingestion such as [4]. However, the model provided in this paper is a simplification by considering meals as glucose ingestions, as done in [2], and taking only

the effect of the size of the meals for gastric emptying.

The model used for glucose absorption in [35] considers only one glucose meal and was used for oral glucose tests in which the patients were given an oral glucose dose and asked to fast while data is collected. The model is given as:

$$\frac{dq_{Ss}}{dt} = -k_{12q}q_{Ss} \tag{1a}$$

$$\frac{dq_{Sl}}{dt} = -k_{\text{empt}}q_{Sl} + k_{12q}q_{Ss} \tag{1b}$$

$$\frac{dq_{\text{int}}}{dt} = -k_{\text{abs}}q_{\text{int}} + k_{\text{empt}}q_{Sl} \tag{1c}$$

$$\begin{aligned} k_{\text{empt}} = k_{\min} + \frac{k_{\max} - k_{\min}}{2}(\\ \tanh\left[\varphi_1\left(q_{Ss} + q_{Sl} - k_{\varphi_1}D_q\right)\right]\\ -\tanh\left[\varphi_2\left(q_{Ss} + q_{Sl} - k_{\varphi_2}D_q\right)\right] + 2) \end{aligned} \tag{1d}$$

$$\varphi_1 = \frac{5}{2D_q(1 - k_{\varphi_1})} \tag{1e}$$

$$\varphi_2 = \frac{5}{2D_q(k_{\varphi_2})} \tag{1f}$$

$$Ra = f_q k_{\text{abs}} q_{\text{int}} \tag{1g}$$

Where $q_{Ss}(0) = D_q$ [mg] is the oral glucose quantity, Ra is the rate of glucose appearance in the blood, f_q is an absorption factor, k_{12} [min^{-1}] and k_{abs} [min^{-1}] are the rate constants for glucose transfer to stomach and glucose absorption in the intestines respectively, k_{empt} [min^{-1}] is a rate parameter for emptying the stomach of glucose to the intestines. This parameter can have values between $k_{\min}$ and $k_{\max}$ depending on the oral glucose quantity D_q. In order to make the model handle different meals with different time instants, the parameter D_q needs to be modified according to the meal sizes and time. The following are the proposed modifications:

$$\frac{dq_{Ss}}{dt} = -k_{12q}q_{Ss} + \sum_{i=1}^{N_q(t)} u_{q_i}\delta(t - t_i), \quad i \in \mathbb{Z}_+ \tag{2a}$$

$$\frac{dD_e}{dt} = -k_q D_e + \sum_{i=1}^{N_q(t)} u_{q_i}\delta(t - t_i) \tag{2b}$$

$$\frac{dD_q}{dt} = k_q\left(u_{q_{N_q(t)}} - D_q\right) + D_m \sum_{i=1}^{N_q(t)} \delta(t - t_i) \tag{2c}$$

$$D_m = \begin{cases} D_e - D_q & u_{q_{N_q(0)}} \neq 0 \\ 1 & u_{q_{N_q(0)}} = 0 \end{cases} \tag{2d}$$

Where $q_{Ss}(0) = 0, D_e(0) = 0$[mg], $\delta(t-t_i)$ is the Dirac delta distribution, t_i is the time instance for meal i, $N_q(t)$ is the integer number of meals until time t starting from time $t = 0$, that is $N_q(t)$ takes into account all meals up until t, u_{q_i} [mg] is the amount of oral carbohydrates intake for meal i. The state D_e is introduced to handle the accumulation of carbohydrates meals with a decay factor k_q [min^{-1}] in order to remove the effect of meals with time. With that, parameter D_q is now a state updated by D_e each time a new meal is consumed and made to converge to the last given meal amount u_{q_i} with the same rate factor k_q such that it converges to the original model through time if no meal is consumed afterwards. Note that $D_q(0) = 0$[mg] when a zero carbohydrates meal ($u_{q_{N_q(0)}} = 0$) is assumed at time $t = 0$, which leads to (1c) being undefined ($\varphi_1 q_{Ss} = \infty$ 0). To avoid this, the state $D_m(0)$[mg] is set to 1[mg] when $u_{q_{N_q(0)}} = 0$. Note also that the value $D_m(0)$ can have any nonzero value in the case of zero carbohydrates meal at $t = 0$. The value $D_m(0)$ will not affect the rate
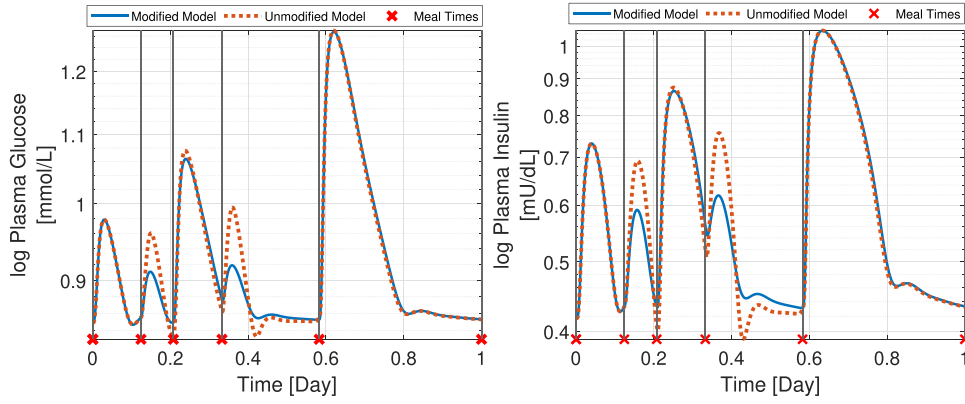
Fig. 2. Simulation results for the modified glucose absorption model against the unmodified one. Note the log scale on the second axis.

of glucose appearance in the plasma since the states q_{Ss} for ingested carbohydrates, and D_e for the effect of accumulation of meals depend on $u_{q_{N_q(0)}}$ and not D_m. Parameters f_q, k_{φ_1}, and k_{φ_2} are known and taken from [9]. The rest of the parameters, k_{12q}, $k_{\min}$, $k_{\max}$, k_{abs}, and k_q are taken to be the mean parameters which were estimated in [35]. The introduced parameter k_q has no estimate. Therefore, it is assumed to be equal to $k_{\min}$.

A simulation of a patient with the modified meals model compared against the unmodified one is shown in Fig. 2. The patient is consuming a breakfast meal of 30 g carbohydrates, a second breakfast meal of 10 g carbohydrates, a lunch meal of 50 g carbohydrates, an afternoon snack of 10 g carbohydrates, and a dinner meal of 110 g carbohydrates. The simulated patient has a basal value of $G_{PC}(0) = 8$ mmol L^{-1} for glucose concentration in the central periphery compartment and $I_{PF}(0) = 1$mU L^{-1} for the insulin concentration in the interstitial fluid periphery compartment. No insulin injections or oral medications, physical activity, or stress are included in this simulation. It can be seen from the simulation results that the glucose appearance in plasma is distributed in a larger window of time with lower peaks for meals that are close to each other. This is due to the reduction of the stomach emptying rate k_{empt} in response to increased accumulation of ingested carbohydrates captured by the state D_q. Additionally, glucose appearance in plasma for the modified model in response to meals after hours of fasting closely resembles the glucose appearance in plasma for the unmodified model as can be seen for the dinner and breakfast meal. This is intended since the unmodified model was proposed for fasting conditions. These observations agree with clinical data such as [27] and [18].

2.2. Insulin injection model

In this section, a model for long acting and fast acting insulin injections based on the one from [23] is introduced to the base model from [10]. Both fast and long acting insulin analogues treatments are considered for the model. When analogue insulin is injected, it dissociates from its hexameric form to dimers and monomers which then can penetrate the capillary membrane and get absorbed into the plasma. For fast acting insulin, only two compartments are considered: a compartment for insulin in its hexameric form, and a compartment for insulin in its dimeric and monomeric form. The following are the equations for fast acting insulin:

$$\frac{dH_{fa}}{dt} = \sum_{i=1}^{N_{fa}(t)} \delta(t - t_i) \frac{10}{V_{PF}^I} u_{f_i}$$

$$- p_{fa}\left(H_{fa} - q_{fa}D_{fa}^3\right) \tag{3a}$$

$$\frac{dD_{fa}}{dt} = p_{fa}\left(H_{fa} - q_{fa}D_{fa}^3\right) - \frac{b_{fa}D_{fa}}{1 + I_{PF}} \tag{3b}$$

Where H_{fa}[mU dL^{-1}] is the concentration of injected fast acting insulin in its hexameric form, D_{fa}[mU dL^{-1}] is the concentration of insulin in its diameric and monomeric form, $N_{fa}(t)$ is the number of injected fast acting insulin doses until time t starting from time $t = 0$, that is $N_{fa}(t)$ takes into account all doses up until t, u_{f_i} [mU] is the amount of injected fast acting insulin, b_{fa} [min^{-1}] is a constant for the infusion of fast acting insulin into the body, p_{fa} [min^{-1}] is a constant diffusion parameter, q_{fa} [dL^2 mU^{-2}] is a constant such that $p_{fa}q_{fa}$ is the parameter for fast acting insulin dimers converting back to hexamers, and I_{PF} [mU dL^{-1}] is the insulin concentration in the interstitial periphery compartment. Parameters for Lispo and Aspart insulin injection are reported in [23]. For long acting insulin, an extra state B_{la} is added in [23] to take into account the increased delay in the dissociation of hexameric insulin to dimers and monomers:

$$\frac{dB_{la}}{dt} = \sum_{i=1}^{N_{la}(t)} \delta(t - t_i) \frac{10}{V_{PF}^I} u_{l_i} - k_{la}B_{la}\frac{C_{\max}}{1 + H_{la}} \tag{4a}$$

$$\frac{dH_{la}}{dt} = k_{la}B_{la}\frac{C_{\max}}{1 + H_{la}} - p_{la}\left(H_{la} - q_{la}D_{la}^3\right) \tag{4b}$$

$$\frac{dD_{la}}{dt} = p_{la}\left(H_{la} - q_{la}D_{la}^3\right) - \frac{b_{la}D_{la}}{1 + I_{PF}} \tag{4c}$$

Where B_{la} [mU dL^{-1}] is the added bound state for the concentration of hexameric insulin before diffusing, H_{la}[mU dL^{-1}] is the concentration of injected long acting insulin in its hexameric form, D_{la}[mU dL^{-1}] is the concentration of injected insulin in its diameric and monomeric form, $N_{la}(t)$ is the number of injected long acting insulin doses until time t starting from time $t = 0$, that is $N_{la}(t)$ takes into account all doses up until t, u_{l_i} [mU] is the amount of long acting insulin dose at time t_i, b_{la} [min^{-1}] is a constant for the infusion of long acting insulin into the body, p_{la} [min^{-1}] is a constant diffusion parameter for long acting insulin, q_{la} [dL^2 mU^{-2}] is a constant such that $p_{la}q_{la}$ is the parameter for long acting insulin dimers converting back to hexamers, k_{la} [min^{-1}] is a constant absorption rate, and $C_{\max}$ is a dimensionless maximum transmission capacity constant. Parameters for insulin Glargin are reported in [23]. The injected insulin enters the interstitial periphery compartment (A.10g) with the following rate r_{Inj}:

$$r_{Inj} = V_{PF}^I \frac{r_{la}b_{la}D_{la}}{1 + I_{PF}} + V_{PF}^I \frac{r_{fa}b_{fa}D_{fa}}{1 + I_{PF}} \tag{5}$$

Where r_{la}, $r_{fa} \leq 1$ are the fractions of long acting and fast acting insulin that get to the periphery compartment, and V_{PH}^I [L] is the volume of the interstitial compartment. Fig. 3 shows a simulation for a patient having the same basal values and following the same meal plan as the simulation discussed in Section 2.1. The patient takes a long acting insulin dose
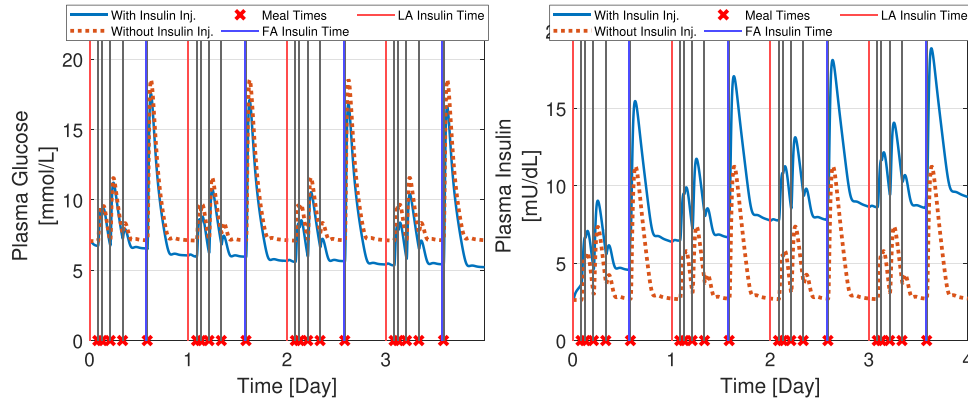
Fig. 3. Simulation showing the effect of injected fast acting (FA) and long acting (LA) insulin on glucose and insulin concentrations.

of 50 [U] everyday an hour before the breakfast meal. Additionally, the patient takes a 30 [U] of fast acting insulin 15 min before dinner. Oral medications, physical activity, and stress are not included in the simulation. Long acting insulin lower the glucose concentration over a large window of time. Moreover, the fast acting insulin helps at reducing the glucose peak after dinner [16]. Quantitative Insulin Sensitivity Check Index (QISCI) [19] is a test performed on fasting glucose and insulin concentrations to assess insulin sensitivity. Healthy patients will typically have values around 0.382 while diabetic patients will have values around 0.304. The QISCI is calculated as:

$$QISCI = \frac{1}{\log(G_{H_f}) + \log(I_{H_f})} \tag{6}$$

Where G_{H_f} and I_{H_f} are the fasting plasma glucose and fasting plasma insulin concentrations respectively. The QISCI was calculated for the case of taking insulin injection doses and for the case in which the patient was not taking any insulin doses. The QISCI with no insulin injections was found to be 0.3717 while the QISCI with insulin injections was found to be 0.3369. The decrease in QISCI agrees with clinical studies [32]. Additionally, the gradual decrease of the glucose concentration during the days with long acting insulin agrees with the data collected in the study in [3].

2.3. Metformin

In this section, a modification for the metformin model in [10] is carried out to account for multiple doses of oral metformin with different amounts. The metformin model used in [10], including the pharmacokinetic and its interaction with full glucose-insulin dynamical models, is based on the model in [34] which was fitted with data from the study in [22] and confirmed with the clinical study in [28]. The pharmacokinetic model of metformin in [34] is given as follows:

$$\frac{dM_{GL}}{dt} = -M_{GL}(k_{go} + k_{gg}) + M_O \tag{7a}$$

$$\frac{dM_{GW}}{dt} = M_{GL}k_{gg} + M_P k_{pg} - M_{GW}k_{gl} \tag{7b}$$

$$\frac{dM_L}{dt} = M_{GW}k_{gl} + M_P k_{pl} - M_L k_{lp} \tag{7c}$$

$$\frac{dM_P}{dt} = M_L k_{lp} - M_P(k_{pl} + k_{pg} + k_{po}) + M_{GL} \tag{7d}$$

Where M_{GL} [µg] is the metformin amount in the gastrointestina lumen, parameters $k_{go}, k_{gg}, k_{pg}, k_{gl}, k_{pl}, k_{lp}, k_{po}$ [min^{-1}] are transfer rate constants between the compartments, and M_O is the flow rate of orally ingested metformin which is modelled as:

$$M_O = Ae^{-\alpha_M t} + Be^{-\beta_M t} \tag{8}$$

Where A, B [µg min^{-1}] and α_M, β_M [min^{-1}] are constant parameters that were identified in [34]. These parameters were identified with data in which patients were taking only a 500 mg oral dose of metformin. Therefore, the model is modified in this work to take into account different amount of doses at different times by introducing the following:

$$\frac{dM_{O1}}{dt} = -\alpha_M M_{O1} + \sum_{i=1}^{N_M(t)} \delta(t - t_i)u_{M_i} \tag{9a}$$

$$\frac{dM_{O2}}{dt} = -\beta_M M_{O2} + \sum_{i=1}^{N_M(t)} \delta(t - t_i)u_{M_i} \tag{9b}$$

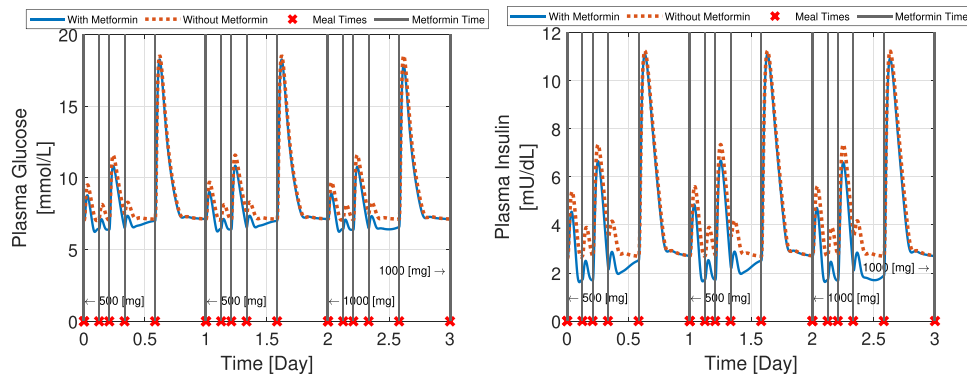$$M_O = \rho_\alpha M_{01} + \rho_\beta M_{02} \tag{9c}$$

Fig. 4. Simulation showing the effect of metformin on glucose and insulin concentrations.
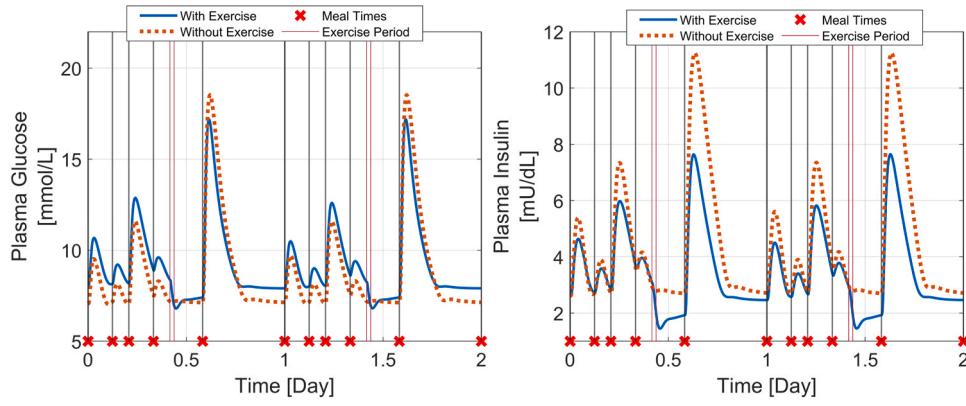
Fig. 5. Simulation showing the effect of physical activity on plasma glucose and plasma insulin concentrations.

with $N_M(t)$ being the number of consumed doses of metformin until time t starting from time $t = 0$, that is $N_M(t)$ takes into account all doses up until t, u_{M_i} [μg] is the amount of metformin consumed at time t_i, and the constants $\rho_\alpha = A/(500000\ [\mu g])$ [min^{-1}] and $\rho_\beta = B/(500000\ [\mu g])$ [min^{-1}] are rate parameters. Fig. 4 shows a simulation result of the same patient as Section 2.1 taking metformin doses of 500 mg for the first two days and then a metformin dose of 1000 mg for the remaining days. Insulin injections, Vildagliptin oral medication, physical activity, and stress are not included in this simulation. The 1000 mg dose prolong the effect of metformin on lowering the glucose concentration when compared to the dose of 500 mg.The effect of metformin on both glucose and insulin concentrations matches the study in [28] that was used to confirm the model in [34]. The QISCI with no metformin doses was found to be 0.3717 while the QISCI with metformin was found to be 0.3921. This shows the effect of metformin improving insulin sensitivity over time.

2.4. Physical activity model

In this section, a physical activity model based on [6] is added to the model in [10]. The model in [6] was developed for a T1D model based on [5]. The model considers the change of the heart beat rate following a physical activity to be the stimulus of two states E_1 and E_2, which are dimensionless:

$$\frac{dE_1}{dt} = -\frac{1}{\tau_{HR}}E_1 + \frac{1}{\tau_{HR}}(HR - HR_b) \tag{10a}$$

$$\frac{dE_2}{dt} = -\left(g_e(E_1) + \frac{1}{\tau_e}\right)E_2 + g_e(E_1) \tag{10b}$$

$$g(E_1) = \frac{\left(\frac{E_1}{a_e HR_b}\right)^{n_e}}{1 + \left(\frac{E_1}{a_e HR_b}\right)^{n_e}} \tag{10c}$$

Where t_{HR}, τ_e min are time constants, HR, HR$_b$bpm are the current and rest heart rates respectively, and the parameters a_e, n_e are dimensionless parameters. The first state E_1 is used directly as a stimulus to increase the insulin-independent glucose uptake in response to a physical activity while the state E_2 is used for the longer lasting change of insulin action on glucose. The glucose and insulin model structure in [6] is simpler than the one considered in this work. Nevertheless, the inclusion of the physical activity for the model in this work is similar to how other models include physical activity, e.g., see [8]. With that, the effect of the state E_1 is included as an increase in the clearance rate of glucose in the periphery interstitial fluid compartment with a constant parameter β_e [bpm^{-1}] as $\frac{1}{T_P^G}(1 + \beta_e E_1)$ where $\frac{1}{T_P^G}$ [min^{-1}] is the clearance rate for glucose in the periphery interstitial fluid compartment in (A.3g). The effect of E_1 can be removed to obtain the original model by setting $\beta_e = 0$. As for the effect on insulin action, the state E_2 is introduced on the glucose metabolic rates, which depend on insulin as follows:

- An increase in the periphery glucose uptake rate r_{PGU} in the interstitial fluid periphery compartment (A.3g) by a constant α_e as $(1 + \alpha_e E_2)r_{PGU}$.
- An increase in the hepatic glucose uptake rate r_{HGU} in the liver compartment (A.3d) with a constant α_e as $(1 + \alpha_e E_2)r_{HGU}$.
- A decrease in the hepatic glucose production rate r_{PGH} in the liver compartment (A.3d) with a constant α_e as $(1 + \alpha_e E_2)r_{HGP}$.
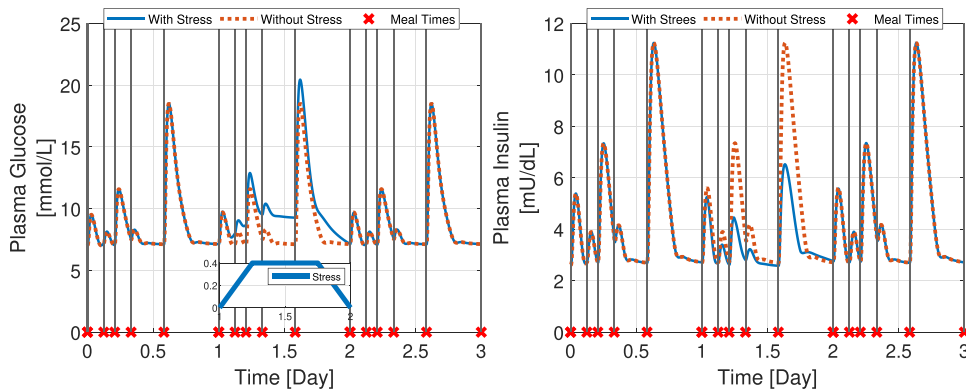

Fig. 6. Simulation showing the effect of stress on glucose and insulin concentrations.

The effect of E_2 can be removed to obtain the original model by setting $\alpha_e = 0$. The parameters for the physical activity model are taken from [6] except for α_e and β_e, which were tuned to have a similar effect to the ones demonstrated in [6,8]. Fig. 5 shows a simulation for the patient described in Section 2.1 when the patient exercise every day before dinner raising the heart beat rate from a rest value of 80bpm to a value of 140bpm for 30 min. Insulin injections, oral medications, and stress are not considered in this simulation. The immediate effect of physical activity is seen in the simulation results. In addition, the prolonged effect of physical activity on insulin action on glucose is seen in the figure.

The QISCI with no physical activity was found to be 0.3717 while the QISCI with physical activity was found to be 0.385. This shows the effect of physical activity on improving the insulin sensitivity.

2.5. Stress effect

In this section, the effect of stress is included in the model [10]. In [11], the effect of stress was included as a multiplicative factor $1 + \alpha_s$, with $\alpha_s \in [0,1]$, to the glucose and glucagon production rates. This is because stress causes a direct increase in the pancreatic glucagon production through an increase in catecholamines, which in turns drives an increase of glucose production in the liver [39]. In addition, stress was also included as a multiplicative factor $1 - \alpha_s$ to the pancreatic insulin secretion rate based on [39]. Similarly, in this work, the effect of stress is included in the model as follows:

- An increase in the plasma glucagon release rate $r_{P\Gamma R}$ in the glucagon compartment (A.9a) as $(1 + \alpha_s)r_{P\Gamma R}$.
- An increase in the hepatic glucose production rate r_{HGP} in the glucose liver compartment (A.3d) as $(1 + \alpha_s)r_{HGP}$.
- A decrease in the pancreatic insulin release rate r_{PIR} in the insulin liver compartment (A.10d) as $(1 - \alpha_s)r_{PIR}$

Fig. 6 shows the effect of stress in a simulation for the same patient discussed in Section 2.1 when the patient is stressed on the second day with α_s ramping up from 0 to 0.4 in 6 h, staying at 0.4 for 12 h, and then ramping down to 0 for the rest of the day. Insulin injections, oral medications, and physical activity are not considered in the simulation. Stress manages to increase glucose concentration together with a decrease in insulin concentration. The QISCI was calculated at fasting conditions after the day in which stress is present. The QISCI with no stress was found to be 0.3717 while the QISCI with stress was found to be 0.3416. This shows a decrease in insulin sensitivity when stress is present for one day.

3. Discussion

3.1. Fitting the model with data

The model has more than 120 parameters and it is, without a doubt, challenging to obtain clinical data that can be used to estimate all the parameters for the model. Nevertheless, the authors in [35], which the model in this paper is based on, performed a sensitivity analysis for the model's parameters and determined a set of specific parameters that are more influential on the response of the model than other. The authors then carried out a least square nonlinear optimization problem to estimate the parameters based on a 50 [g] oral glucose tolerance test data in which peripheral glucose and insulin concentrations are measured together with incretin concentration. Since the model in this paper is based on the one in [35], patients can perform oral glucose tolerance test occasionally to obtain data which, can be used to estimate personalized parameters for the base model. Subsequently, the estimated parameters for the base model can be fixed for each patient while the parameters for the extensions of the base model can be estimated using data that can be collected during the treatment process of the patients. Data for stress can be collected using the Perceived Stress Scale (PSS) as done in the studies

[1,26] in which a self-administered questionnaire is filled by the patients. Afterwards, a stress level can be deduced from the answers by mapping them to be between 0 and 1 to match the model presented in this paper. As for the physical activity model, heart beat rate data can be acquired using wearable smart watches as discussed in [30]. Together with these data, continues glucose measurement data with registered insulin injections and oral medications data can be used to estimate more parameters of the augmented models other than the base model parameters.

3.2. Usage of the model

In this section, it is intended to discuss examples on how the model can be used to help subjects with Type 2 diabetes. Consider a patient who performed oral glucose tolerance test to estimate the base model parameters and has been providing data during treatment to estimate parameters of the augmented sub-models. Assume now a case in which the patient is expected to have a stressful period of 4 days. For examples, a school exam period. From previously gathered data about stress, the patient is expected to have stress levels ranging from 0.4 to 0.8 during these days. Moreover, the eating patterns of the patients are fitted from previously collected meal registered data according to the following for each meal of the day:

with $\mathscr{U}(a,b)$ being a continues uniform distribution between a and b. In addition, the patient is known to have physical activity every day from to 16:00–16:30 raising their heart beat rate by 40 [bpm]. With all these information, a medical professional can test different treatment plans for the patient using the model by performing a Monte Carlo simulation with the given information about the patient. Fig. 7 shows a Monte Carlo simulation for a treatment plan consisting of long acting insulin doses of 40[U] at the beginning of each day together with metformin doses of 500 [mg] each day. The patient has a basal value of $G_{PC}(0) = 8$ mmol L^{-1} for glucose concentration in the central periphery compartment and $I_{PF}(0) = 1$mU L^{-1} for the insulin concentration in the interstitial fluid periphery compartment. It is seen from the figure that the fasting glucose is brought to a safe glucose concentration region between 4 and 6 for some simulations. Nevertheless, it is seen that for some cases the patient can experience high glucose concentration levels during the meals. The medical professional now test a different treatment plan where the metformin dose is increased to 1000 [mg] and the long acting insulin dose is increased to 50 [U]. Fig. 8 shows the results. It can be seen now that the new treatment plan produces simulations with lower glucose concentration peaks. The example shows how the model gives the opportunity for a medical professional to test different treatment plans against the combined effect of different factors such as stress and physical activity for patients.

Fig. 7. 1000 Simulations of the patient with stress levels drawn uniformly between 0.4 and 0.8 for each simulation and a meal plan according to Table 1. The patient is taking a long acting insulin dose of 40[U] and a metformin dose of 500[mg] each day of the simulation.
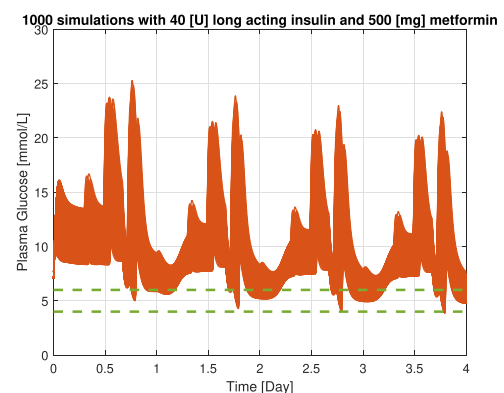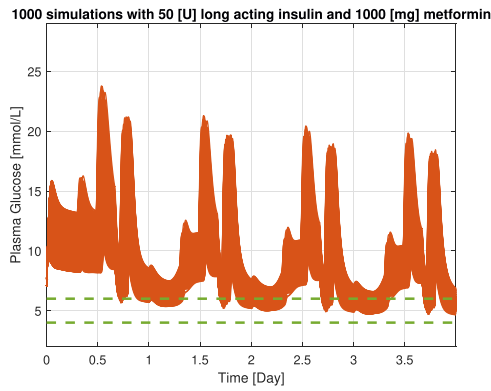
Fig. 8. 1000 Simulations of the patient with stress levels drawn uniformly between 0.4 and 0.8 for each simulation and a meal plan according to Table 1. The patient is taking a long acting insulin dose of 50[U] and a metformin dose of 1000[g] each day of the simulation.

The model can also be used to evaluate the performance of dose finding algorithms for insulin injections or oral medications against different kinds of patients and different lifestyles with stress, physical activity, and meals. For example, consider the rule based strategy for determining long acting insulin doses based on fasting glucose measurement in [40]. The dose finder's goal is to bring and keep fasting glucose concentrations within a safe region between 4 [mmol/L] and 5 [mmol/L]. Fig. 9 shows the results of applying the rule based long acting insulin dose finding strategy to three different hypothetical patients to test the robustness of the strategy. The first patient having the same parameters as in Table B.3. The second patient is chosen to have the same parameters as in Table B.3 except with parameters c_1 and c_4 increased by 90% and c_2 decreased by 90%. This was done to increase the effect of insulin on the metabolic glucose uptake and glucose production rates. Finally, the third patient is chosen to have the same parameters as in Table B.3 except with parameters c_1 and c_4 decreased by 90% and c_2 increased by 90%. This was done to decrease the effect of insulin on the metabolic glucose uptake and glucose production rates. Note that the 90% increase or decrease on the parameters is chosen arbitrary. The parameter perturbation range in which one can use for the parameters of the model and still obtain a model that represent a real life patient is uncertain. Nevertheless, ensuring a strategy to be robust under extreme cases is still an advantage. All the patients have meal plans identical to Table 1. In addition, all the patients are taking a metformin dose of 500 [mg] and having physical activity each day from 16 to 16:30 increasing their heart beat rate during that period to 40 [bpm]. The aim of these simulations is to test the robustness of the dose finding algorithm against physiologically different patients. It can be seen from the
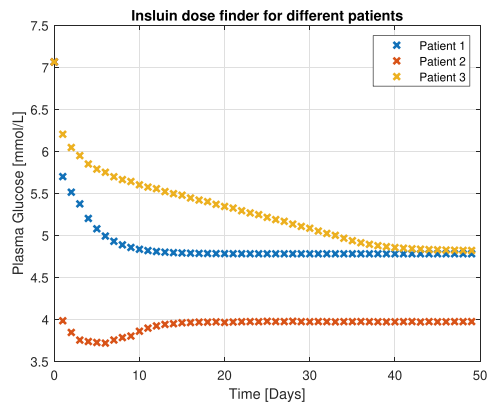
Table 1
Meals model for the hypothetical patient.

Meal	Time [Hours]	Glucose [g]
Breakfast	$\mathcal{U}(7,8)$	$\mathcal{U}(5,40)$
Lunch	$\mathcal{U}(11.5,13)$	$\mathcal{U}(50,100)$
Dinner	$\mathcal{U}(17,19)$	$\mathcal{U}(100,130)$

figure that the strategy managed to bring the fasting glucose concentrations for patient 1 to be within a safe range in less than 10 days. For patient 3, the strategy needed more time to bring the fasting glucose concentrations to the safe region. As for patient 2, the strategy undershoot below the safe region and then converged to a value on the lower limit of the safe region. This is dangerous since the risk of hypoglycemic episodes are higher for patient 2. In conclusion, the strategy can handle a variety of patients with different insulin resistivity. Nevertheless, the strategy can take a long period to have the fasting glucose concentrations converging for some cases. Moreover, it can cause patients to experience hypoglycemia by undershooting or converging to a concentration on the lower limit for the safe region, which is dangerous.

This evaluation study was tested with the effect of physical activity considerations and metformin medication. Consider now testing the same strategy with the same patients but without the consideration of physical activity and metformin. Fig. 10 shows the results. It is clear from the figure that the strategy performs differently. While none of the patients risk experiencing hypoglycemia, the strategy takes more time to converge for all of them. Another point to notice here is that patient 2 now takes more time to converge to the safe region than patient 3. The possibility to perform evaluations of treatment plans against physical activity and stress together with other medications is what distinguish this model from the current state of the art models.

The model can also be used to design insulin and oral medication dose finders for patients. For example, similarly to how the model is used in the first example to test and evaluate treatment plans, the model can be used in an optimization algorithm to decide on the insulin, oral medication doses, or even physical activity conditions. Such strategies are refereed to as optimal predictive controllers or model predictive controller (MPC). One can use robust MPC techniques such as [20] by choosing a compact set in which some of the model parameters can take values from. In this case, one can optimize for certain objectives, e.g. bringing glucose concentrations to a safe region, or minimizing the use of injected insulin, while insuring satisfaction of some constraints, e.g. limited amounts of insulin, allowed time for physical activity, or constraining glucose concentrations to a specific region, for all possible values of the chosen parameters in the compact set. Moreover, one can have a more relaxed and realistic version by choosing a probability for
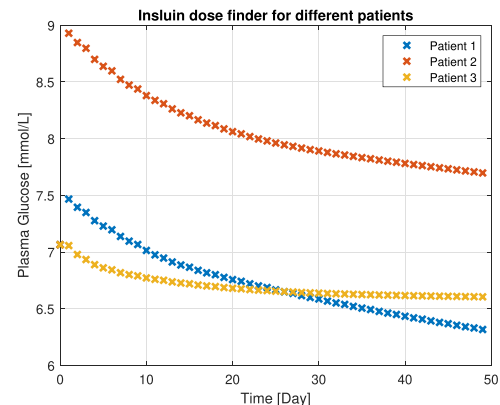

Fig. 9. Fasting Glucose for three different patients. Physical activity and a dose of 500 [mg] metformin are considered.

Fig. 10. Fasting Glucose for three different patients. Physical activity and metformin are not considered.

the parameters to be inside the chosen compact set (Robust with probability MPC), and thus, ensuring the constraint satisfaction with a specific probability value. Another option is to consider stochastic MPC techniques [13] to handle stochastic disturbances or inputs similar to the meal plan example in Table 1. Stochastic MPC techniques offers the chance to optimize for the expected values of objectives or the probabilities of objective while ensuring the satisfaction of some constraints with some chosen probability.

4. Conclusion and future work

A model for glucose-insulin dynamics, which incorporates the effect of multiple glucose meal sizes, different metformin doses, physical activity, insulin injections, and stress, is proposed by combining and modifying different available models in the literature. The effect of the different added and modified models is demonstrated by different simulations and was aimed to match studies from the literature on T2D patients. A discussion on the data needed to fit the model is provided. Additionally, a discussion is provided on how the model can be used to evaluate treatment plans and possibly develop some treatment plans with robust and stochastic control techniques. The model, however, need to be confirmed with real patients data. Moreover, real patient data can be used to estimate joint probability distribution to simulate a population of T2D patients.

CRediT authorship contribution statement

Mohamad Al Ahdab: Conceptualization, Methodology, Software, Formal analysis, Writing - Original Draft, Visualization. **John Leth:** Project administration, Supervision, Writing - Review & Editing. **Torben Knudsen:** Supervision, Writing - Review & Editing. **Peter Vestergaard:** Validation, Writing - Review & Editing. **Henrik Glavind Clausen:** Writing - Review & Editing.

Declaration of Competing Interest

The authors declare that they have no known competing financial interests or personal relationships that could have appeared to influence the work reported in this paper.

Acknowledgements

Appendix A. Full model equations

The compartments include metabolic production rates r_{CXP} and metabolic uptake rates r_{CXU} for substance X in compartment C generally defined as following:

$$r_{CXP,U} = M^I M^G M^\Gamma r^b_{CXP,U} \tag{A.1}$$

Where M^I, M^G, and M^Γ are multiplicative quantities for the effect of insulin I, glucose G, and glucagon Γ respectively, and $r^b_{CXP,U}$ is the basal metabolic rate of substance X in compartment C. The general form for the multiplicative quantities representing the effect of a substance Y in compartment C with concentration Y_C is given as:

$$M^Y = \frac{a + b\tanh\left[c\left(Y_C/Y^b_C - d\right)\right]}{a + b\tanh[c(1 - d)]} \tag{A.2}$$

Where Y^b_C is the basal concentration of substance Y in compartment C, and a, b, c, and d are model parameters.

A.1. Glucose Sub-Model

Applying mass balance equations over the compartments for glucose, the following equations are obtained:

$$V^G_{BC}\frac{dG_{BC}}{dt} = Q^G_B(G_H - G_{BC}) - \frac{V^G_{BF}}{T^G_B}(G_{BC} - G_{BF}) \tag{A.3a}$$

$$V^G_{BF}\frac{dG_{BF}}{dt} = \frac{V^G_{BF}}{T^G_B}(G_{BC} - G_{BF}) - r_{BGU} \tag{A.3b}$$

$$V^G_H\frac{dG_H}{dt} = Q^G_B G_{BC} + Q^G_L G_L + Q^G_K G_K$$
$$+ Q^G_P G_{PC} + Q^G_H G_H - r_{RBCU} \tag{A.3c}$$

$$V^G_G\frac{dG_G}{dt} = Q^G_G(G_H - G_G) - r^m_{GGU} + Ra \tag{A.3d}$$

$$V^G_L\frac{dG_L}{dt} = Q^G_A G_H + Q^G_G G_G - Q^G_L G_L$$
$$+ \left((1 + \alpha_s)(1 - \alpha_e E_2)r^m_{HGP} - (1 + \alpha_e E_2)r_{HGU}\right) \tag{A.3e}$$

$$V^G_K\frac{dG_K}{dt} = Q^G_K(G_H - G_K) - r_{KGE} \tag{A.3f}$$

$$V^G_{PC}\frac{dG_{PC}}{dt} = Q^G_P(G_H - G_{PC}) - \frac{V^G_{PF}}{T^G_P}(G_{PC} - G_{PF}) \tag{A.3g}$$

$$V_{PF}^G \frac{dG_{PF}}{dt} = \frac{V_{PF}^G}{T_P^G}(G_{PC})$$
$$- (1 + \beta_e E_1)G_{PF}) - (1 + \alpha_e E_2)r_{PGU}^m$$

$$(A.3h)$$

Where G_i[mg dL^{-1}] is glucose concentration for each compartment i, Q_i^G [dL min^{-1}] is the vascular blood flow for the glucose compartment i, V_i^G [dL] is the volume of compartment i, T_i^G [min] is the transcapillary diffusion time for compartment i, and r_{xP}, r_{xU} are metabolic glucose production and uptake rates respectively. The following are the meanings of each subscript in the model: Table A.2.

Table A.2
Subscripts abbreviations.

B	Brain	BC	Brain capillary space
BF	Brain interstitial fluid	H	Heart
G	Guts	L	Liver
K	Kidney	P	Periphery
PC	Periphery capillary space	PF	Periphery interstitial fluid
BGU	Brain glucose uptake	RBCU	Red blood cell glucose uptake
GGU	Gut glucose uptake	HGP	Hepatic glucose production
HGU	Hepatic glucose uptake	KGE	Kidney glucose excretion
PGU	Peripheral glucose uptake		

The metabolic rates for the glucose subsystem are given as:

$$r_{PGU} = M_{PGU}^I M_{PGU}^G r_{PGU}^b, \quad r_{PGU}^b = 35 \tag{A.4a}$$

$$r_{HGP} = M_{HGP}^I M_{HGP}^G M_{HGP}^\Gamma r_{HGP}^b, \quad r_{HGP}^b = 35 \tag{A.4b}$$

$$r_{HGU} = M_{HGU}^I M_{HGU}^G r_{HGU}^b, \quad r_{HGU}^b = 20 \tag{A.4c}$$

$$r_{KGE} = \begin{cases} 71 + 71\tanh[0.11(G_K - 460)] & G_K < 460 \\ -330 + 0.872G_K & G_K \geq 460 \end{cases} \tag{A.4d}$$

$$r_{BGU} = 70, \quad r_{RBCU} = 10, \quad r_{GGU} = 20 \tag{A.4e}$$

Where:

$$M_{PGU}^I = \frac{7.03 + 6.52\tanh[c_1(I_{PF}/I_{PF}^B - d_1)]}{7.03 + 6.52\tanh[c_1(1 - d_1)]} \tag{A.5a}$$

$$M_{PGU}^G = G_{PF}/G_{PF}^b \tag{A.5b}$$

$$\frac{d}{dt}M_{HGP}^I = 0.04(M_{HGP}^{I\infty} - M_{HGP}^I) \tag{A.5c}$$

$$M_{HGP}^{I\infty} = \frac{1.21 - 1.14\tanh[c_2(I_L/I_L^B - d_2)]}{1.21 - 1.14\tanh[c_2(1 - d_2)]} \tag{A.5d}$$

$$M_{HGP}^G = \frac{1.42 - 1.41\tanh[c_3(G_L/G_L^B - d_3)]}{1.42 - 1.41\tanh[c_3(1 - d_3)]} \tag{A.5e}$$

$$M_{HGP}^\Gamma = 2.7\tanh[0.39\Gamma/\Gamma^B] - f \tag{A.5f}$$

$$\frac{d}{dt}f = 0.0154\left[\left(\frac{2.7\tanh[0.39\Gamma/\Gamma^B] - 1}{2}\right) - f\right] \tag{A.5g}$$

$$\frac{d}{dt}M_{HGU}^I = 0.04(M_{HGU}^{I\infty} - M_{HGU}^I) \tag{A.5h}$$

$$M_{HGU}^{I\infty} = \frac{2.0\tanh[c_4(I_L/I_L^B - d_4)]}{2.0\tanh[c_4(1 - d_4)]} \tag{A.5i}$$

$$M_{HGU}^G = \frac{5.66 + 5.66\tanh[c_5(G_L/G_L^B - d_5)]}{5.66 + 5.66\tanh[c_5(1 - d_5)]} \tag{A.5j}$$

Note that some of these rates have a constant numerical value. In addition, parameters a and b for the multiplicative quantities are substituted with numerical values. These numerical values are the ones estimated for a healthy 70 kg male. Parameters c and d were left for the estimation in case of a

diabetic patient as in [35]. The following rates are modified with the effect of metformin as following:

$$r_{GGU}^{m} = (1 + E_{GW})r_{GGU} \tag{A.6a}$$

$$r_{HGP}^{m} = (1 - E_{L})r_{HGP} \tag{A.6b}$$

$$r_{PGU}^{m} = (1 + E_{P})r_{PGU} \tag{A.6c}$$

Where E_{GW}, E_L, and E_P are positives coefficients which depend on the amount of metformin in the gastrointestina wall (GI) M_{GW} [μg], liver M_L [μg], and peripherals M_p [μg] respectively. These coefficients increase (or decrease) the glucose uptake (or production) as seen in (A.6). The equations for these coefficients are given as following:

$$E_{GW} = \frac{\nu_{GW,\text{max}} \times (M_{GW})^{n_{GW}}}{\left(\varphi_{GW,50}\right)^{n_{GW}} + (M_{GW})^{n_{GW}}} \tag{A.7a}$$

$$E_{L} = \frac{\nu_{L,\text{max}} \times (M_{L})^{n_{L}}}{\left(\varphi_{L,50}\right)^{n_{L}} + (M_{L})^{n_{L}}} \tag{A.7b}$$

$$E_{P} = \frac{\nu_{P,\text{max}} \times (M_{P})^{n_{P}}}{\left(\varphi_{P,50}\right)^{n_{P}} + (X_{P})^{n_{P}}} \tag{A.7c}$$

Where $\nu_{GW,\text{max}}$, $\nu_{L,\text{max}}$, $\nu_{P,\text{max}}$ are parameters to represent the maximum effect of metformin in each one of its corresponding compartments, $\varphi_{GW,50}$, $\varphi_{GI,50}$, $\varphi_{GI,50}$ [μg] are the masses of metformin within the different compartments to produce half of its maximum effect, and n_{GW}, n_L, and n_P are shape factors.

A.2. Incretins Sub-Model

The incretins hormones are metabolic hormones released after eating a meal to stimulate a decrease in blood glucose levels. For T2D patients, Glucagon-Like-Peptide-1 (GLP-1) is the most active incretin [12]. GLP-1 is then modelled with the following two compartments as in [10]:

$$\frac{d\psi}{dt} = \zeta k_{\text{empt}}q_{Sl} - \frac{1}{\tau_{\psi}}\psi \tag{A.8a}$$

$$V^{\Psi}\frac{d\Psi}{dt} = \frac{1}{\tau_{\psi}}\psi - [K_{out} + (R_{maxC} - DR_c)Cf_2]\Psi \tag{A.8b}$$

Where τ_{ψ} [min^{-1}] is a time constant for the release and absorption of GLP-1 to the blood stream upon consuming a meal, V^{Ψ}[dL] is the volume of the GLP-1 compartment, DR_c[nmol] is the amount of Dipeptidyl peptidase-4 (DPP-4) in the central compartment deactivated by the drug vildagliptin, K_{out} [min^{-1}] is a clearance constant for GLP-1 independently of the amount of DPP-4, and $(R_{maxC} - DR_c)$ is the amount of available activated DPP-4 in the blood plasma with R_{maxC}[nmol] being the maximum amount of active DPP-4 in the absence of the vildagliptin. Cf_2 [min^{-1} nmol^{-1}] is a proportionality factor for the elimination of GLP-1 by active DPP-4 [21]. Parameters τ_{ψ} and ζ are estimated in [35] when other incretins than GLP-1 are considered and later modified in [35] to account for vildagliptin treatment. Parameters K_{out}, R_{maxC}, and Cf_2 were estimated in [21] together with the parameters for the vildagliptin model described in subsection Appendix A.6.

A.3. Glucagon Sub-Model

The glucagon subsystem consists of one compartment as it is assumed to have the same concentration over all the body:

$$V^{\Gamma}\frac{d\Gamma}{dt} = (1 + \alpha_s)r_{P\Gamma R} - 9.1\Gamma \tag{A.9a}$$

$$r_{P\Gamma R} = M_{P\Gamma R}^{G}M_{P\Gamma R}^{I}r_{P\Gamma R}^{b}, \quad r_{P\Gamma R}^{b} = 9.1 \tag{A.9b}$$

$$M_{P\Gamma R}^{G} = 1.31 - 0.61\tanh\left[1.06\left(\frac{G_H}{G_H^B} - 0.47\right)\right] \tag{A.9c}$$

$$M_{P\Gamma R}^{I} = 2.93 - 2.09\tanh\left[4.18\left(\frac{I_H}{I_H^B} - 0.62\right)\right] \tag{A.9d}$$

Where $r_{P\Gamma R}$ is the plasma glucagon release rate. The state Γ represent a normalized glucagon state with respect to its basal value. This is done since it is difficult in practice to obtain glucagon measurements for each subject in order to initialize the state. Therefore for this model, the basal glucagon state is 1.

A.4. Insulin Sub-Model

Applying mass balance equations over the insulin compartments will yield the following:

$$V_B^I \frac{dI_B}{dt} = Q_B^I(I_H - I_B) \tag{A.10a}$$

$$V_H^I \frac{dI_H}{dt} = Q_B^I I_B + Q_L^I I_L + Q_K^I I_K$$
$$+ Q_P^I I_{PV} - Q_H^I I_H \tag{A.10b}$$

$$V_G^I \frac{dI_G}{dt} = Q_G^I(I_H - I_G) \tag{A.10c}$$

$$V_L^I \frac{dL_L}{dt} = Q_A^I I_H + Q_G^I I_G - Q_L^I I_L$$
$$+ (1 - \alpha_s)r_{PIR} - r_{LIC} \tag{A.10d}$$

$$V_K^I \frac{dI_K}{dt} = Q_K^I(I_H - I_K) - r_{KIC} \tag{A.10e}$$

$$V_{PC}^I \frac{dI_{PC}}{dt} = Q_P^I(I_H - I_{PC}) - \frac{V_{PF}^I}{T_P^I}(I_{PC} - I_{PF}) \tag{A.10f}$$

$$V_{PF}^I \frac{dI_{PF}}{dt} = \frac{V_{PF}^I}{T_P^I}(I_{PC} - I_{PF}) - r_{PIC} + r_{Inj} \tag{A.10g}$$

Where r_{LIC}, r_{KIC}, and r_{PIC} are the liver, kidney, and peripherals insulin clearance rates respectively and are defined as following:

$$r_{LIC} = 0.4\left[Q_A^I I_H + Q_G^I I_G - Q_L^I I_L + r_{PIR}\right] \tag{A.11a}$$

$$r_{KIC} = 0.3Q_K^I I_K \tag{A.11b}$$

$$r_{PIC} = \frac{I_{PF}}{\left[\left(\frac{1-0.15}{0.15Q_P^I}\right) - \frac{20}{V_{PF}^I}\right]} \tag{A.11c}$$

the pancreas insulin release is calculated by the following:

$$r_{PIR} = \frac{S}{S^b}r_{PIR}^b \tag{A.12}$$

Where S [U min^{-1}] is the pancreas secreted insulin rate, and S^b, r_{PIR}^b are the basal values. The model for S and S^b is described in subsection Appendix A.5.

A.5. Pancreas Sub-Model

The model consists of two main compartments: a large insulin storage compartment m_s [µg] and a small labile insulin compartment m_l [µg]. The flow of insulin from the storage compartment to the labile insulin compartment is dependent on a dimensionless factor P with a proportionality constant γ [µg min^{-1}]. The factor P depends on a dimensionless glucose-enhanced excitation factor represented by X and GLP-1 through a linear compartment with constant first order rate α [min^{-1}]. Upon a glucose stimulus, the glucose-enhanced excitation factor X will increase instantaneously depending on the glucose increase in the plasma G_H. In addition, a dimensionless inhibitor R for X will increase in response to X through a linear compartment with a first order constant rate β [min^{-1}]. During that increase, the secreted insulin S will depend directly on both X and its inhibitor R together with GLP-1. Afterwards when R reaches X or X starts decreasing after R reaching it, the insulin secretion rate will only depend on X and GLP-1. The following are the equations of the model:

$$\frac{dm_s}{dt} = K_l m_l - K_s m_s - \gamma P \tag{A.13a}$$

$$\frac{dm_l}{dt} = K_s m_s - K_l m_l + \gamma P - S \tag{A.13b}$$

$$\frac{dP}{dt} = \alpha(P_\infty - P) \tag{A.13c}$$

$$\frac{dR}{dt} = \beta(X - R) \tag{A.13d}$$

$$S = \begin{cases} [N_1 P_\infty + N_2(X - R) + \zeta_2 \Psi]m_l & X > R \\ (N_1 P_\infty + \zeta_2 \Psi)m_l & X \le R \end{cases} \tag{A.13e}$$

$$P_\infty = X^{1.11} + \zeta_1 \Psi \tag{A.13f}$$

$$X = \frac{G_H^{3.27}}{132^{3.27} + 5.93 G_H^{3.02}} \tag{A.13g}$$

Where K_l [min^{-1}] and K_s [min^{-1}] are the rates for the flow between the labile and storage insulin compartments independently of P, N_1 [min^{-1}] and N_2 [min^{-1}] are constant parameters that represent the effect of P and $(X - R)$ on the insulin secretion rate respectively, and ζ_1 [L pmol^{-1}], ζ_2 [L (pmol min)$^{-1}$] are constant parameters to represent the effect of GLP-1 on P_∞ and the insulin secretion rate. For initializing the model and calculating the basal values, the storage compartment is assumed to be large enough for it to be constant. Therefore, writing the mass balance for the storage compartment at zero glucose concentration will yield the following:

$$K_s m_s = K_l m_{l_0} \tag{A.14}$$

Where m_{l_0} is the labile insulin concentration at zero glucose concentration. This parameter in [33] is provided with a value of 6.33[U] for a healthy 70 kg male.

A.6. Vildagliptin

The vildagliptin model is based on [21]. The absorption of orally ingested vildagliptin is modelled by two compartments as following:

$$\frac{dA_{G1}}{dt} = -k_{a1}A_{G1} + \sum_{i=1}^{N_v(t)} \delta(t - t_i)f_v u_{v_i} \tag{A.15a}$$

$$\frac{dA_{G2}}{dt} = k_{a1} \times A_{G1} - k_{a2} \times A_{G2} \tag{A.15b}$$

Where A_{G1}, A_{G2} [nmol] are the amount of vildagliptin in the gut and absorption compartments respectively, $N_v(t)$ is the number of oral vildagliptin doses until time t, u_{v_i} [nmol] is the amount of consumed vildagliptin, f_a is the bioavailability of vildagliptin, and k_{a1}, k_{a2} [min^{-1}] are rate absorption parameters. After that, the model contains a central and a peripheral compartment for the vildagliptin and the vildagliptin-DPP-4 complex (deactivated DPP-4):

$$\begin{aligned} \frac{dA_c}{dt} &= k_{a2}A_{G2} - \frac{CL + CL_{ic}}{V_C}A_C + \frac{CL_{ic}}{V_p}A_p \\ &- \frac{(R_{\max C} - DR_C)k_{v2}\frac{A_c}{V_C}}{K_{vd} + \frac{A_c}{V_c}} + k_{off}DR_C \end{aligned} \tag{A.16a}$$

$$\begin{aligned} \frac{dA_p}{dt} &= CL_{ic}\left(\frac{A_c}{V_c} - \frac{A_p}{V_p}\right) \\ &- \frac{(R_{\max P} - DR_P)k_{v2}\frac{A_p}{V_p}}{K_{vd} + \frac{A_p}{V_p}} + k_{off}DR_P \end{aligned} \tag{A.16b}$$

$$\begin{aligned} \frac{dDR_C}{dt} &= \frac{(R_{\max C} - DR_C)k_{v2}\frac{A_C}{V_C}}{K_{vd} + \frac{A_C}{V_C}} \\ &- (k_{off} + k_{deg})DR_C \end{aligned} \tag{A.16c}$$

$$\begin{aligned} \frac{dDR_P}{dt} &= \frac{(R_{\max P} - DR_P)k_{v2}\frac{A_P}{V_P}}{K_{vd} + \frac{A_P}{V_P}} \\ &- (k_{off} + k_{deg})DR_P \end{aligned} \tag{A.16d}$$

Where A_C, A_P nmol are the amounts of vildagliptin in the central and peripheral compartments respectively, CL [L min^{-1}] is a non-saturable clearance, CL_{ic} [L min^{-1}] is the inter-compartmental clearance, V_c, V_p [L] are the volumes of the central and peripheral compartments respectively, k_{v2} [min^{-1}] is a parameter added for the slow tight binding of vildagliptin to DPP-4, K_{vd} [nmol L^{-1}] is the equilibrium dissociation constant, k_{off} [min^{-1}] is a rate constant for the dissociation of intact vildagliptin from DPP-4, R_{maxP} [nmol] is the maximum possible amount of DPP-4 in the peripheral compartment, k_{deg} [min^{-1}] is a rate constant for the hydrolysis of vildagliptin by DPP-4, and DR_P [nmol] is the amount of deactivated DPP-4 in the peripheral compartments.

Appendix B. Parameter mean values

Table B.3 includes the values of the parameters which were used in the simulation.

Table B.3
Parameter values.

Parameter	Value	Parameter	Value	Parameter	Value
V_{BC}^G [dL]	3.5	V_{BF}^G [dL]	4.5	V_H^G [dL]	13.8
V_L^G [dL]	25.1	V_G^G [dL]	11.2	V_K^G [dL]	6.6
V_{PC}^G [dL]	10.4	V_{PF}^G [dL]	67.4	V_B^I [L]	0.26
V_H^I [L]	0.99	V_G^I [L]	0.94	V_L^I [L]	1.14
V_K^I [L]	0.51	V_{PC}^I [L]	0.74	V_{PF}^I [L]	6.74
V^Γ [mL]	6.74	Q_B^G [dL min^{-1}]	5.9	Q_H^G [dL min^{-1}]	43.7
Q_A^G [dL min^{-1}]	2.5	Q_L^G [dL min^{-1}]	12.6	Q_G^G [dL min^{-1}]	10.1
Q_K^G [dL min^{-1}]	10.1	Q_P^G [dL min^{-1}]	15.1	Q_B^I [L min^{-1}]	0.45
Q_H^I [L min^{-1}]	3.12	Q_A^I [L min^{-1}]	0.18	Q_K^I [L min^{-1}]	0.72
Q_P^I [L min^{-1}]	1.05	Q_G^I [L min^{-1}]	0.72	Q_L^I [L min^{-1}]	0.9
T_B^G [min]	2.1	T_P^G [min]	5.0	T_P^I [min]	20.0
f_q [·]	0.9	$k_{\phi1}$ [·]	0.68	$k_{\phi2}$ [·]	0.00236
k_{12_q} [min^{-1}]	0.08	k_{min} [min^{-1}]	0.005	k_{max} [min^{-1}]	0.05
k_{abs} [min^{-1}]	0.08	c_1 [·]	0.067	c_2 [·]	1.59
c_3 [·]	0.62	c_4 [·]	1.72	c_5 [·]	2.03
d_1 [·]	1.126	d_2 [·]	0.683	d_3 [·]	0.14
d_4 [·]	0.023	d_5 [·]	1.59	m_{l_0} [U]	6.33
ζ_1 [Lpmol^{-1}]	0.0026	ζ_2 [L (pmolmin^{-1})]	0.99e^{-4}	K_l [min^{-1}]	0.3621
K_s [min^{-1}]	0.0572	γ [μg min^{-1}]	2.366	α [min^{-1}]	0.615
β [min^{-1}]	0.931	N_1 [min^{-1}]	0.0499	N_2 [min^{-1}]	0.00015
V^ψ [dL]	11.31	K_{out} [min^{-1}]	68.3041	Cf_2 [min^{-1} nmol^{-1}]	21.1512
τ_ψ [min^{-1}]	35.1	R_{maxC} [nmol]	5.0	ζ [·]	8.248
f_v [·]	0.772	k_{a1} [min^{-1}]	0.021	k_{a2} [min^{-1}]	0.0175
CL [L min^{-1}]	0.6067	CL_{ic} [L min^{-1}]	0.6683	V_p [L]	97.3
k_{off} [min^{-1}]	0.0102	R_{maxP} [nmol]	13	k_{deg} [min^{-1}]	0.0018
V_c [L]	22.2	K_{vd} [nmol L^{-1}]	71.9	k_{v2} [min^{-1}]	0.39
k_{go} [min^{-1}]	1.88e–4	k_{gg} [min^{-1}]	1.85e–4	k_{pg} [min^{-1}]	4.13
k_{gl} [min^{-1}]	0.46	k_{pl} [min^{-1}]	0.00101	k_{lp} [min^{-1}]	0.91
k_{po} [min^{-1}]	0.51	$\nu_{GW,max}$ [·]	0.9720	$\nu_{L,max}$ [·]	0.7560
$\nu_{P,max}$ [·]	0.2960	n_{GW} [·]	2.0	n_L [·]	2.0
n_P [·]	5.0	$\phi_{GW,50}$ [·]	431.0	$\phi_{L,50}$ [·]	521.0
$\phi_{P,50}$ [·]	1024.0	ρ_α [min^{-1}]	54	ρ_β [min^{-1}]	54
α_M [min^{-1}]	0.06	β_M [min^{-1}]	0.1	p_{la} [min^{-1}]	0.5
r_{la} [·]	0.2143	q_{la} [dL^2 mU^{-2}]	3.04e^{-10}	b_{la} [min^{-1}]	0.025
C_{max} [·]	15.0	k_{la} [min^{-1}]	2.35e^{-5}	p_{fa} [min^{-1}]	0.5
r_{fa} [·]	0.2143	q_{fa} [dL^2 mU^{-2}]	1.3e^{-11}	b_{fa} [min^{-1}]	0.0068
τ_{HR} [min]	5.0	n_e [·]	4.0	a_e [·]	0.8
τ_e [min]	600	α_e [·]	2.974	β_e [bpm^{-1}]	3.39e–4

References

[1] A.J. Ahola, C. Forsblom, V. Harjutsalo, P.H. Groop, Perceived stress and adherence to the dietary recommendations and blood glucose levels in type 1 diabetes, J. Diabetes Res. 2020 (2020).

[2] T.B. Aradóttir, D. Boiroux, H. Bengtsson, J. Kildegaard, B.V. Orden, J.B. Jørgensen, Model for simulating fasting glucose in type 2 diabetes and the effect of adherence to treatment, IFAC-PapersOnLine 50, 20th IFAC World Congress, (2017) 15086–15091.

[3] T.B. Aradóttir, H. Bengtsson, M.L. Jensen, N.K. Poulsen, D. Boiroux, L.L. Jensen, S. Schmidt, K. Nørgaard, Feasibility of a new approach to initiate insulin in type 2 diabetes, J. Diabetes Sci. Technol. (2020).

[4] T. Arleth, S. Andreassen, M. Orsini-Federici, A. Timi, M. Massi-Benedetti, A model of glucose absorption from mixed meals, IFAC Proc. Vol. 33 (2000) 307–312.

[5] R.N. Bergman, Y.Z. Ider, C.R. Bowden, C. Cobelli, Quantitative estimation of insulin sensitivity, Am. J. Physiol. Endocrinol. Metab. 236 (1979), E667.

[6] M.D. Breton, Physical activity—the major unaccounted impediment to closed loop control, (2008).

[7] C. Cobelli, C. Dalla Man, G. Sparacino, L. Magni, G. De Nicolao, B.P. Kovatchev, Diabetes: models, signals, and control, IEEE Rev. Biomed. Eng. 2 (2009) 54–96.

[8] C. Dalla Man, M.D. Breton, C. Cobelli, Physical activity into the meal glucose—insulin model of type 1 diabetes: in silico studies, (2009).

[9] C. Dalla Man, R.A. Rizza, C. Cobelli, Meal simulation model of the glucose-insulin system, IEEE Trans. Biomed. Eng. 54 (2007) 1740–1749.

[10] M. Eftekhari, O. Vahidi, Mechanism based pharmacokinetic pharmacodynamic modeling of vildagliptin as an add-on to metformin for subjects with type 2 diabetes, Comput. Model. Eng. Sci. 114 (2018) 153–171.

[11] L. Gaohua, H. Kimura, A mathematical model of brain glucose homeostasis, Theor. Biol. Med. Model. 6 (2009).

[12] A.J. Garber, Incretin therapy–present and future, Rev. Diabet. Stud. RDS 8 (2011) 307.

[13] E. González, J. Sanchis, S. García-Nieto, J. Salcedo, A comparative study of stochastic model predictive controllers, Electronics 9 (2020) 2078.

[14] J. Hunt, I. MacDonald, The influence of volume on gastric emptying, J. Physiol. 126 (1954) 459–474.

[15] International Diabetes Federation. IDF Diabetes Atlas, 9 ed., International Diabetes Federation, Brussels, Belgium, 2019.

[16] F.S.T. Investigators, et al., Glucose variability in a 26-week randomized comparison of mealtime treatment with rapid-acting insulin versus glp-1 agonist in participants with type 2 diabetes at high cardiovascular risk, Diabetes Care 39 (2016) 973–981.

[17] H.I. Jacoby, Gastric emptying. Reference Module in Biomedical Sciences, Elsevier, 2017.

[18] D. Jakubowicz, J. Wainstein, B. Ahren, Z. Landau, Y. Bar-Dayan, O. Froy, Fasting until noon triggers increased postprandial hyperglycemia and impaired insulin response after lunch and dinner in individuals with type 2 diabetes: a randomized clinical trial, Diabetes Care 38 (2015) 1820–1826.

[19] A. Katz, S.S. Nambi, K. Mather, A.D. Baron, D.A. Follmann, G. Sullivan, M.J. Quon, Quantitative insulin sensitivity check index: a simple, accurate method for assessing insulin sensitivity in humans, J. Clin. Endocrinol. Metab. 85 (2000) 2402–2410.

[20] J. Köhler, M.A. Müller, F. Allgöwer, A novel constraint tightening approach for nonlinear robust model predictive control, in: Proceedings of the 2018 Annual American Control Conference (ACC), (2018) pp. 728–734.

[21] C.B. Landersdorfer, Y.L. He, W.J. Jusko, Mechanism-based population modelling of the effects of vildagliptin on glp-1, glucose and insulin in patients with type 2 diabetes, Br. J. Clin. Pharmacol. 73 (2012) 373–390.

[22] S.H. Lee, K.i. Kwon, Pharmacokinetic-pharmacodynamic modeling for the relationship between glucose-lowering effect and plasma concentration of metformin in volunteers, Arch. Pharmacal Res. 27 (2004) 806–810.

[23] J. Li, J.D. Johnson, Mathematical models of subcutaneous injection of insulin analogues: a mini-review, Discret. Contin. Dyn. Syst. Ser. B 12 (2009) 401.

[24] R.J. Mahler, M.L. Adler, Type 2 diabetes mellitus: update on diagnosis, pathophysiology, and treatment, J. Clin. Endocrinol. Metab. 84 (1999) 1165–1171.

[25] MATLAB, version R2020a. The MathWorks Inc., Natick, Massachusetts, (2020).

[26] A. Mishra, V. Podder, S. Modgil, R. Khosla, A. Anand, R. Nagarathna, R. Malhotra, H.R. Nagendra, Higher perceived stress and poor glycemic changes in prediabetics and diabetics among indian population, J. Med. Life 13 (2020) 132.

[27] M.J. Munsters, W.H. Saris, Effects of meal frequency on metabolic profiles and substrate partitioning in lean healthy males, PLoS One 7 (2012), e38632.

[28] L. Pala, E. Mannucci, I. Dicembrini, C. Rotella, A comparison of mealtime insulin aspart and human insulin in combination with metformin in type 2 diabetes patients, Diabetes Res. Clin. Pract. 78 (2007) 132–135.

[29] M. Rashid, S. Samadi, M. Sevil, I. Hajizadeh, P. Kolodziej, N. Hobbs, Z. Maloney, R. Brandt, J. Feng, M. Park, et al., Simulation software for assessment of nonlinear and adaptive multivariable control algorithms: glucose–insulin dynamics in type 1 diabetes, Comput. Chem. Eng. 130 (2019), 106565.

[30] B. Reeder, A. David, Health at hand: a systematic review of smart watch uses for health and wellness, J. Biomed. Inform. 63 (2016) 269–276.

[31] R.M. Røge, S. Klim, N.R. Kristensen, S.H. Ingwersen, M.C. Kjellsson, Modeling of 24-hour glucose and insulin profiles in patients with type 2 diabetes mellitus treated with biphasic insulin aspart, J. Clin. Pharmacol. 54 (2014) 809–817.

[32] D. Šimonienė, A. Platūkienė, E. Prakapienė, L. Radzevičienė, D. Veličkiene, Insulin resistance in type 1 diabetes mellitus and its association with patient's micro- and macrovascular complications, sex hormones, and other clinical data, Diabetes Ther. Res. Treat. Educ. Diabetes Relat. Disord. 11 (2020) 161–174.

[33] J.T. Sorensen, A Physiologic Model of Glucose Metabolism in Man and its use to Design and Assess Improved Insulin Therapies for Diabetes (Ph.D. thesis), Massachusetts Institute of Technology, 1985.

[34] L. Sun, E. Kwok, B. Gopaluni, O. Vahidi, Pharmacokinetic-pharmacodynamic modeling of metformin for the treatment of type ii diabetes mellitus, Open Biomed. Eng. J. 5 (2011) 1.

[35] O. Vahidi, K. Kwok, R.B. Gopaluni, F. Knop, A comprehensive compartmental model of blood glucose regulation for healthy and type 2 diabetic subjects, Med. Biol. Eng. Comput. 54 (2016) 1383–1398.

[36] R. Visentin, C. Cobelli, C. Dalla Man, The padova type 2 diabetes simulator from triple-tracer single-meal studies: in silico trials also possible in rare but not-so-rare individuals, Diabetes Technol. Ther. 22 (2020) 892–903.

[37] R. Visentin, M. Schiavon, C. Dalla Man, In silico cloning of target type 2 diabetes population for treatments development and decision support, in: Proceedings of the 2020 42nd Annual International Conference of the IEEE Engineering in Medicine & Biology Society (EMBC), IEEE, (2020) pp. 5111–5114.

[38] K. Wong, D. Glovaci, S. Malik, S.S. Franklin, G. Wygant, U. Iloeje, H. Kan, N. D. Wong, Comparison of demographic factors and cardiovascular risk factor control among u.s. adults with type 2 diabetes by insulin treatment classification, J. Diabetes Complicat. 26 (2012) 169–174.

[39] S. Woods, D. Porte Jr, E. Bobbioni, E. Ionescu, J. Sauter, F. Rohner-Jeanrenaud, B. Jeanrenaud, Insulin: its relationship to the central nervous system and to the control of food intake and body weight, Am. J. Clin. Nutr. 42 (1985) 1063–1071.

[40] B. Zinman, A. Philis-Tsimikas, B. Cariou, Y. Handelsman, H.W. Rodbard, T. Johansen, L. Endahl, C. Mathieu, N.B.O.L.T. Investigators, et al., Insulin degludec versus insulin glargine in insulin-naive patients with type 2 diabetes: a 1-year, randomized, treat-to-target trial (begin once long), Diabetes Care 35 (2012) 2464–2471.